UNIVERSITY OF CALIFORNIA

Los Angeles

The Use of Holographic Interferometry for Measurements of Temperature in a Rectangular Heat Pipe

Department of Mechanical, Aerospace and Nuclear Engineering
School of Engineering and Applied Science
University of California, Los Angeles

by

Jure Marn

In Partial Satisfaction for the Degree of

Master of Science

1989

CONTENTS

LIST OF FIGURES

ACKNOWLEDGMENTS

Thanks to my commitee chair, Dr. Ivan Catton, for his guidance and advice. This work was supported by NASA Lewis under Contract No. NAG3-899 and NASA Dryden under Contract No. NCC2-374 Supp 2. I would also like to thank the other people who have helped me in various ways: Farrokh Issacci, Mo Chung and Parham Adnani.

Chapter I

INTRODUCTION

A. HOLOGRAPHIC INTERFEROMETRY

Holographic Interferometry is a non-intrusive optical method and as such posesses considerable advantages. It does not disturb the velocity and temperature field by creating an obstacles which would alter the flowfield. Their contribution to the total energy of the system may be negligible, in comparison with the amounts of energy transported within the system by natural processes. Further, there are practically no inertial errors.This contributes to flexibility and enables us to observe transient processes, which would otherwise be hard to observe. Moreover, the measurement technique simultaneously deals with a large portion of the flowfield (with the same interferogram), avoiding point-by-point measurements.

These (optical) methods have some disadvantages as well. First, the apparatus requires a steady powerful source of single wavelength (coherent) light, i.e. laser. Second, some techniques require pre and postprocessing of emitted and reflected light, e.g. Laser Doppler Anemometry or special optics, e.g. Mach-Zender cells. Third, these techniques cannot be easily performed and require high quality components, e.g. special coated lenses etc. Therefore a desirable

interferometry technique should overcome these difficulties and still retain the accuracy and other advantages of above methods.

Holography, as one of the interferometry methods, retains the accuracy of older methods, and at the same time eliminated the system error of participating components. It also allows one to adjust the measurement technique to the experiment being performed; e.g. the speed of recording and speed of data processing.

There are, unfortunately, still some disadvantages in holography. The measured media must be transparent, as well as the borders (the walls) of the experiment. This often brings problems due to different physical characteristics of glass (as most common used housing) when compared to the the properties of the experimental media. Furthermore, although a considerable portion of fluid field is recorded simultaneously, one is limited by the strength of spatial filters and collimators and intensity of the beams. The results obtained are not straigthforward, they have to be processed and this allows the possibility of either wrong interpretation or human error.

The holographic interferometry consists of comparing the objective beam with the reference beam and observing the difference in lengths of optical paths, which can be observed during the propagation of the light through a medium with locally varying refractive index. Thus, change in the refractive index can be observed as a family of nonintersecting surfaces in space

(wave fronts), described with an eikonal equation with E = const. The eikonal (geometrical wave front) equations can be obtained by describing light propagation through a three dimensional vector field with streamlines being the light rays. A more detailed description of the process and the equations are given in /1/.

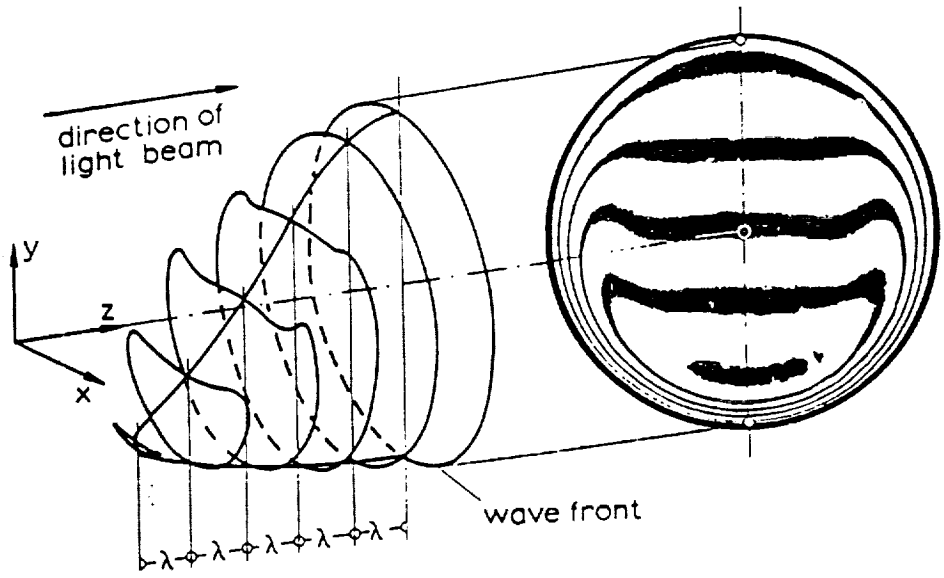

Figure 1: The Interferogram of the Wave Front /1/

The portrayal of wave front as a surface in space is seen in the figure 1. The phase difference, caused by the structure of wave front, while the light is passing through the surface affects changes in intensity of the light and

therefore makes the boundaries of each eikonal surface visible. There are two types of interference possible:

1. Normal Interference (Mach-Zehnder): If the light beam is passed through a distorted wave front, and its recording is compared to some reference (undistorted) wave front, the difference is seen in terms of interference lines. The contours, seen in the figure 1, are intersections between parallel equidistant plane surfaces (S and λ) and the distorted wave front. Here λ represents wavelength of the light beam we are measuring with, S being an integer positive multiplier. For odd multiples of $\lambda/2$, a minima in intensity occurs and for even multiples, a maxima occurs. Mimima is represented with black stripes whereas maxima with brighter (more intensive) lines.
2. Differential Interference: If the same wave front is displaced laterally, parallel to the direction of the light beam, the difference in displacement can be observed as a change in refractive index and therefore by means of interference lines.

B. HEAT PIPE

The object of our investigation is a rectangular heat pipe. This device is used for transfer of heat by evaporating and condensing the working fluid. A wick structure is used to return the condensed fluid to the evaporator employing capillary forces in the wick.The capillary forces must yield

sufficient transfer of the vapor from the evaporator to condenser. The latent heat of evaporation is exploited by the evaporating on the heated side and condensing on the coolde side.

There are many advantages to the heat pipes. It is compact, can be made modular and can achieve very high effective thermal conductivity. It can be used in many environments with excess heat production, where space and weight limitations exist. Such environments exist in space vehicles. fusion energy systems and electronic appliances.

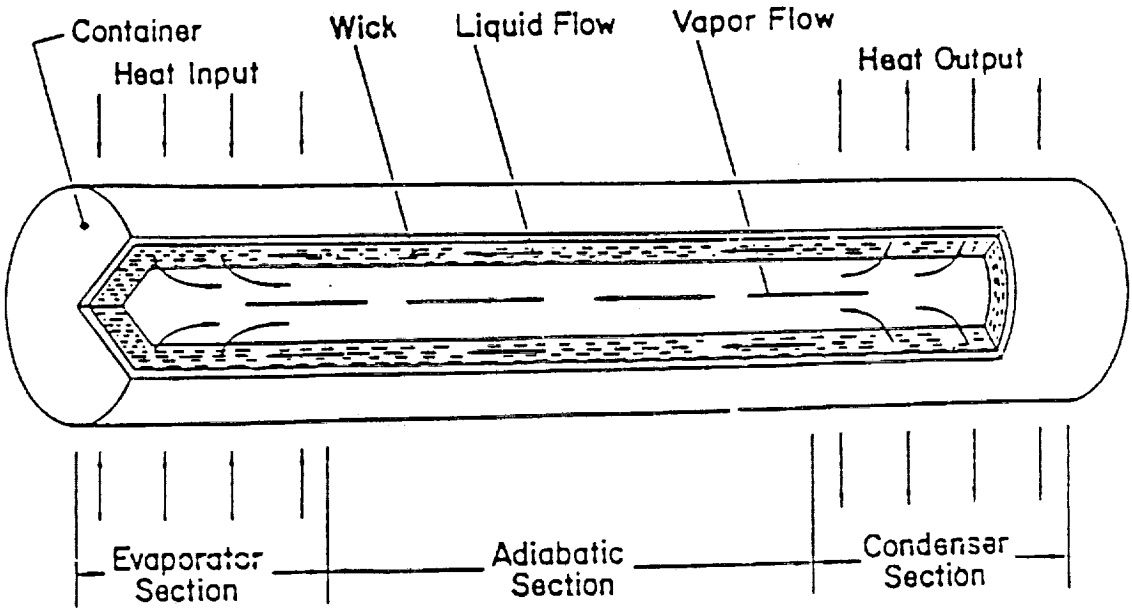

Figure 2: A Heat Pipe /2/

Figure 2 shows the heat pipe, which consists of a case, a wick structure, and a vapor space. Our experiment simulates an axisymetric crossection of the heat pipe in figure. In order to justify this simplification we have assumed the gravity forces to be small compared to convective forces. This can be justified knowing the fact that vapor velocities in heat pipes sometimes approach the sonic velocity. Another assumption was that the fluid layer is thin and horizontal, therefore the gravity forces in the fluid layer can be neglected. The rectangular shape of the experimental heat pipe is therefore justified.

Gaugler /3/ developed the concept of a heat pipe to cool the interior of an ice box. Later, an intensive work was performed by Grover et al./4/ at Los Alamos National Laboratory. The first quantitative analysis was performed by Cotter /5/ in 1965. Since then there have been many advances in theory, design and practice of heat pipes.

Chapter II

THE THEORY ON HOLOGRAPHIC INTERFEROMETRY

A. SINGLE BEAM INTERFEROMETRY

To avoid confusion with the literature /1/, a single beam will denote single wavelength measurements, although actually two beams will be used. The emitting source isa laser. The laser beam is split into an object beam and a reference beam. The optical system needed to do this is placed on an air suspensed table. The reason for the use of a "floating" table is the sensitivity of the measurement method to any disturbance from the surroundings, e.g. vibrations, caused by someone walking through the lab or an elevator in use.

Results are obtained using two beams of the same wavelength but with a phase difference due to change in the refractive index of a disturbed system. A 4W water cooled laser with an ethalon (to secure a blue beam at 460 nm) is used. The beam is led through an objective lense (40:1) and then collimated to maintain parallel direction while passing through the measurement section. The layout of the apparatus is displayed in figure 3 for the single beam interferometry where the change in refractive index due to a dominant variation in the property field. Refractive index is, in general, a function of temperature and density and is a material property. If we want

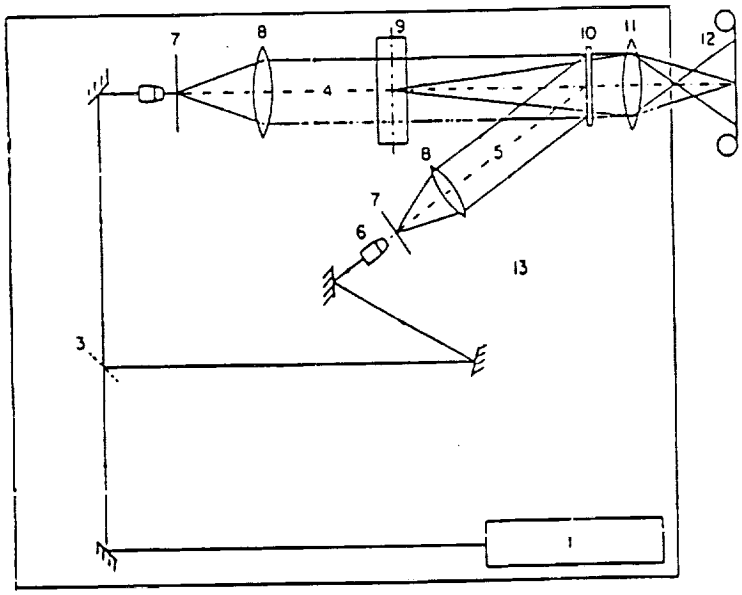

Figure 3: The Apparatus for Single Beam Holography Interferometry
1. Laser, 3. Variable Beam Splitter, 4. Object Beam,
5. Reference Beam, 6. Spatial Filter, 7.Pinhole,
8. Collimating Lens, 9. Test Section,
10. Holographic Plate, 11. Lens, 12. Camera,
13. Air Suspension Table, 14. Shutter

to measure only the temperature gradient, then we have to make sure that we are dealing with a pure material at constant density. In this case, the difference in refractive index is expressed as:

$$S(x,y,t)\ \lambda = l\ \Delta n(\lambda) \tag{1}$$

If, for example, the temperature field is dominates. equation (1) can be written

$$S(x,y,t)\ \lambda = l\ \frac{\partial n(\lambda)}{\partial T}\ \Delta T \qquad (2)$$

Clearly, one can deduce a similar equation for the concentration field at constant temperature. The techniques used for actual measurements and derivation of equations will be described as a part of a more general description of twin beam interferometry, as proposed by Mayinger and Panknin /6/.

B. TWIN BEAM INTERFEROMETRY

In practice problems with one substance only are seldom present. Normally, one is dealing with a mixture in a temperature field. To use holographic interferometry, one must take advantage of the fact that changes in the refractive indices do not depend only upon the disturbances in the field measured, but also upon the wavelength of the light we are measuring with. This idea was thoroughly explored by Panknin /7/. He has used the concept of twin beam holography to obtain good results in measurements of the temperature and concentration along a heated ablated vertical wall.

To implement twin beam interferometry, the existing apparatus used for single beam interferometry was upgraded by adding a 15 mW red (He-Ne) laser, with wavelength λ = 632.8 nm.

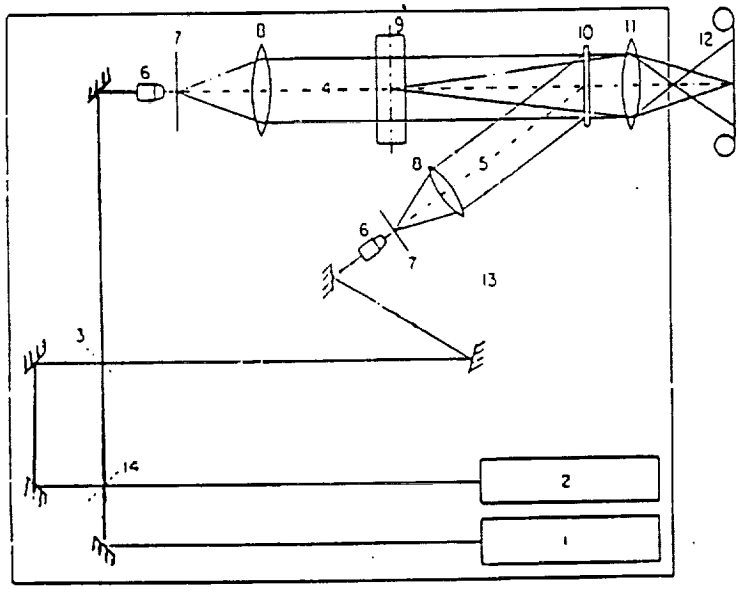

Figure 4: The Apparatus for Twin Beam Holography Interferometry
1,2. Lasers, 3. Variable Beam Splitter, 4. Object Beam,
5. Reference Beam, 6. Spatial Filter, 7.Pinhole,
8. Collimating Lens, 9. Test Section,
10. Holographic Plate, 11. Lens, 12. Camera,
13. Air Suspension Table, 14. Shutter

The photographic recording method for twin beam holography, see figure 4, is different from that used in single beam interferometry. There, the hologram was recorded and then compared with the observed distorted field. In this case the hologram is recorded with both lasers simultaneously,

with their beams carefully aligned on the same spot. To obtain the needed results, interference fringes are obtained using each beam separately. The two sets of fringes yield two equation and two unknowns allowing one to obtain temperature or concentration field.

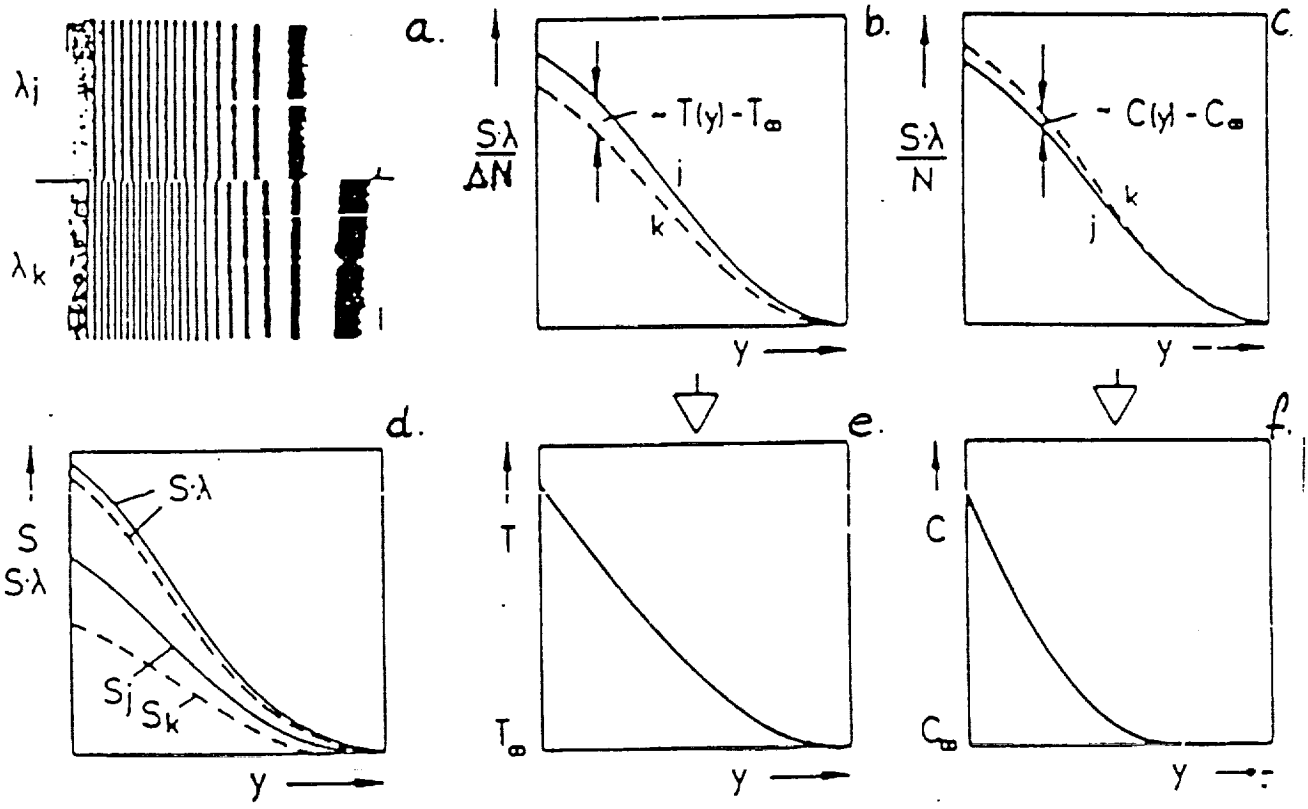

Figure 5: The Twin Beam Holography Output

Figure 5 /6/ describes the procedure followed to obtain results, recorded via twin beam technique. In order to calculate actual data, we have to supply actual data on material used and derive equations used.

C. THE THEORY OF TWIN BEAM INTERFEROMETRY

The following assumptions are made in the development of the governing equations /7/:

1. The optical system is perfect, the experimental setup is mechanically stable, and the lasers are ideal.
2. The object beams with the wavelengths λ_j and λ_k are ideal parallel waves.
3. The variation of refractive index is only two dimensional.
4. There is no reflection of the beam due to gradients of the refractive index.
5. The refractive index of the environment and of the test section (while recording comparison waves) is constant.
6. The holographic construction is perfect.

We have assumed that the density is either constant or it is changing linearly with temperature. Now, with the possibility of recording results at different wavelengths, one can deduce a system of equations for as many unknowns as we have wavelengths. However, since the change of refractive index is conditioned with temperature and concentration field, we need to employ two different wavelengths as mentioned before. The object beam, passing through the test section at different times, is superimposed on the comparison wave, which is observed as the difference in optical lenghts of two exposures. This can be expressed in multiples S of the wavelength λ

$$S(x,y,\lambda) = l[n(x,y,\lambda) - n_{\infty}] \tag{3}$$

where l is the length of the test section in which the refractive index varies. As a matter of fact, with that approach we observe an average index change over the test section. To determine the change at a point, one must consider the distance between two fringes as a length of the test section.

An extinction of light (dark fringes) occurs for

$$|S| = \frac{1}{2}, \frac{3}{2}, \frac{5}{2}, \cdots \tag{4}$$

and amplification (bright fringes) for

$$|S| = 1, 2, 3, \cdots \tag{5}$$

Interference fringes are points of having the same refractive index change and can be associated with the points of the same temperature or concentration. To relate change of refractive index to change of temperature and concentration, one must find the "neutral" material property which depends only on material and wavelength of light used. Such a property is the molar refractivity $N(\lambda)$, which is related to the refractive index by Lorenz- Lorenz equation:

$$N(\lambda) = \frac{n(\lambda)^2 - 1}{n(\lambda)^2 + 2} \frac{M}{\rho} \tag{6}$$

For the gases with refraction index $n \cong 1$, equation (6) can be approximated by the Gladstone - Dale equation:

$$N(\lambda) = \frac{2M}{3\rho}[n(\lambda) - 1] \tag{7}$$

If one makes the further assumption that the working gas is be nearly ideal, M/ρ can be replaced with the total pressure p , temperature T , and universal gas constant, R , to yield

$$N(\lambda) = \frac{2RT}{3p}[n(\lambda) - 1] \tag{8}$$

For a mixture of gases. the molar refractivity is given by a linear combination of the molar refractivities of the components, weighted by their concentration

$$N(\lambda) = \sum_{m=1}^{q} C_m N_m \tag{9}$$

where q is total number of components in the mixture. Note also that

$$\sum_{m=1}^{q} C_m = 1 \tag{10}$$

Equations (3) and (8) yield the following expression

$$S_i\lambda_i = \frac{3}{2}\,\frac{lp}{R}\left[\frac{1}{T_i}\sum_{m=1}^{q} C_{mi}N_{mi} - \frac{1}{T_\infty}\sum_{m=1}^{q} C_{mi\infty}N_{mi\infty}\right] \tag{11}$$

Assuming $q = 2$ one can write the following equation, omitting the independant variables while describing the dependant variables,

$$S_i\lambda_i = \frac{3}{2}\frac{lp}{R}\left\{\frac{1}{T}[C_a(N_a - N_b) + N_b]\frac{1}{T_\infty}[C_a(N_{a\infty} - N_{b\infty}) + N_{b\infty}]\right\} \quad (12)$$

Since $N_a = N(\lambda)$, $N = N_\infty$ yielding

$$S_i\lambda_i = \frac{3lp}{2R}\left[N_a\left(\frac{C_a}{T} - \frac{C_{a\infty}}{T_\infty}\right) + N_b\left(\frac{C_a + 1}{T} - \frac{C_{a\infty}}{T_\infty}\right)\right] \quad (13)$$

with

$$\Delta N_j \equiv N_a(\lambda_j) - N_b(\lambda_j) \quad (14)$$

the final form of equations, used for determination of temperature and concentration in the flow field, become

$$T - T_\infty = \frac{S_j\lambda_j}{\Delta N_j} - \frac{S_k\lambda_k}{\Delta N_k} \quad (15)$$

and

$$C - C_\infty = \frac{S_j\lambda_j}{N_j} - \frac{S_k\lambda_k}{N_k} \quad (16)$$

1. The Single Beam Equations

The single beam equations, with use of which the temperatures or concentrations can be measured, are special cases of the twin beam equations. A single beam can be employed under the assumption that concentration of all the other ingredients are equal to zero, or that we are

interested only in the gas mixture (which is uniform) and not its components. In this case, equation (13) becomes

$$S\ \lambda = \frac{3Ip}{2R}\ N(\lambda)\left(\frac{1}{T} - \frac{1}{T_\infty}\right) \tag{17}$$

and finally

$$\frac{1}{T} = \frac{1}{T_\infty} + \frac{2}{3}\ \frac{S\lambda R}{IpN} \tag{18}$$

or, if we want to calculate the concentration with $T = const$

$$C = C_\infty + \frac{2}{3}\ \frac{S\lambda RT}{IpN} \tag{19}$$

All of the equations above are derived for what is called the infinite mode. To illustrate the infinite mode, a picture of a burning candle is shown in figure 6. The fringes on the picture sre showing the column of almost uniform temperature above the flame and very steep temperature gradient to the sides.

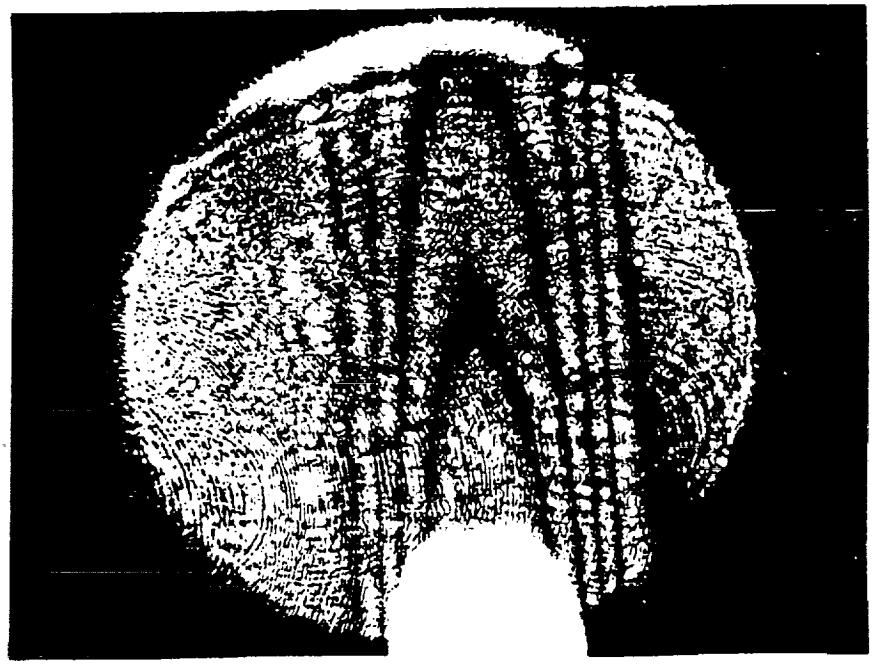

Figure 6: The Infinite Fringes of the Candle Flame

2. The Finite Mode Single Beam Equations

For finite fringes, the system of calculations is somewhat different. To achieve the finite fringes mode, the system is initially disturbed by changing some of its important physical parameters. During the present experiments this was achieved by changing the properties of the spatial filter. In this case there are two reference temperatures, one arbitrarily set, and one at which the initial state is recorded. The advantage of this method is that although the molar refractivity is still a function of the wavelength and material properties, one does not have to look it up in the tables - it is

determined by the initial state of the system, i.e. by the initial number of the finite fringes. In that case (18) becomes

$$\frac{1}{T} = \frac{1}{T_\infty} + \frac{2}{3}\,\frac{S\lambda R}{lpN_{fin}} \tag{20}$$

This yields

$$N_{fin} = \frac{2}{3}\,\frac{S_{fin}\lambda R}{lp}\,\frac{TT_\infty}{T_\infty - T} \tag{21}$$

where T is actual temperature and T_∞ is an arbitrarily set temperature, typically set equal to the boiling temperature. We can employ N_{fin} instead of our previous molar refractivity in equations (18) and (19) to calculate temperature and concentration respectively.

As an example of finite fringes two pictures, one showing the candle flame and the other the actual heat pipe in steady state mode of operation, are shown in fihures 7 and 8. Although the physical picture of the phenomena on the picture 7 is not as accurate as on figure 6, it is better noticeable. The condensation layer in figure 8 could be seen with the use of infinite mode as well, however it can be easily observed in the finite mode. The temperature gradient in the figure 8 is represented by the angle of the fringes rather than with their density.

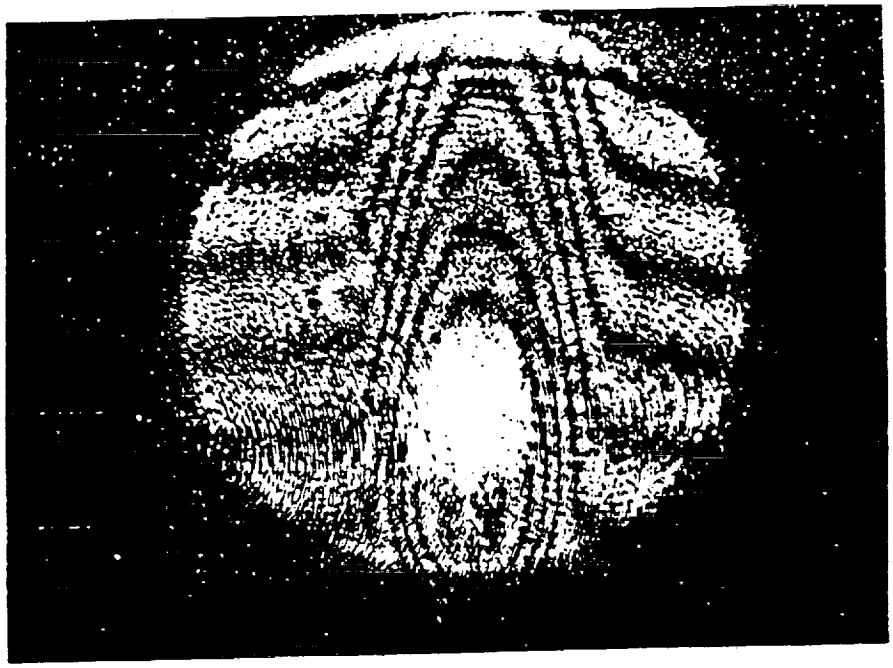

Figure 7: The Finite Fringes Around the Candle Flame

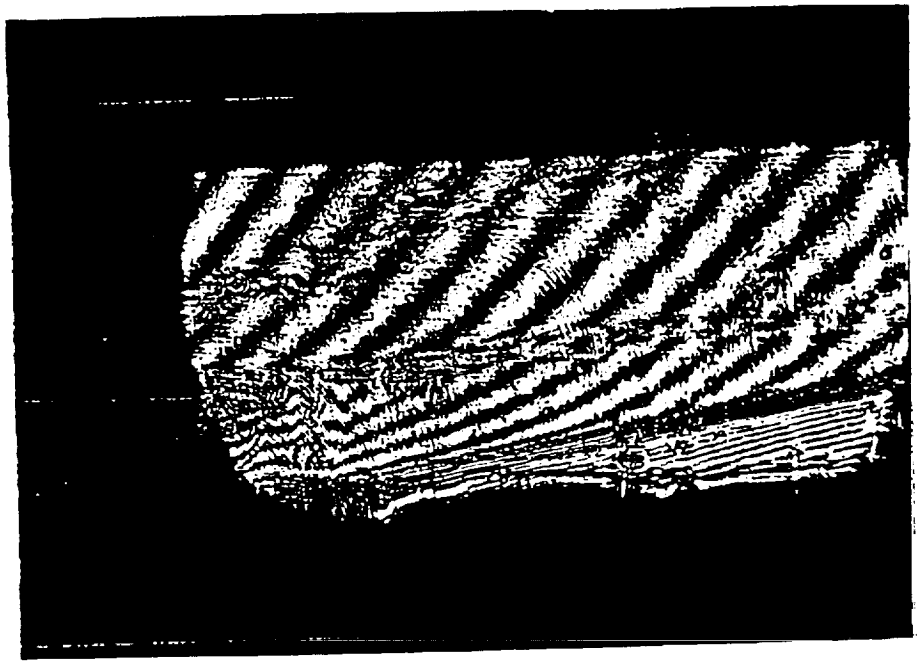

Figure 8: The Finite Fringes in the Heat Pipe

Chapter III

THE EXPERIMENT

The rectangular heat pipe is shown in the figure 9.

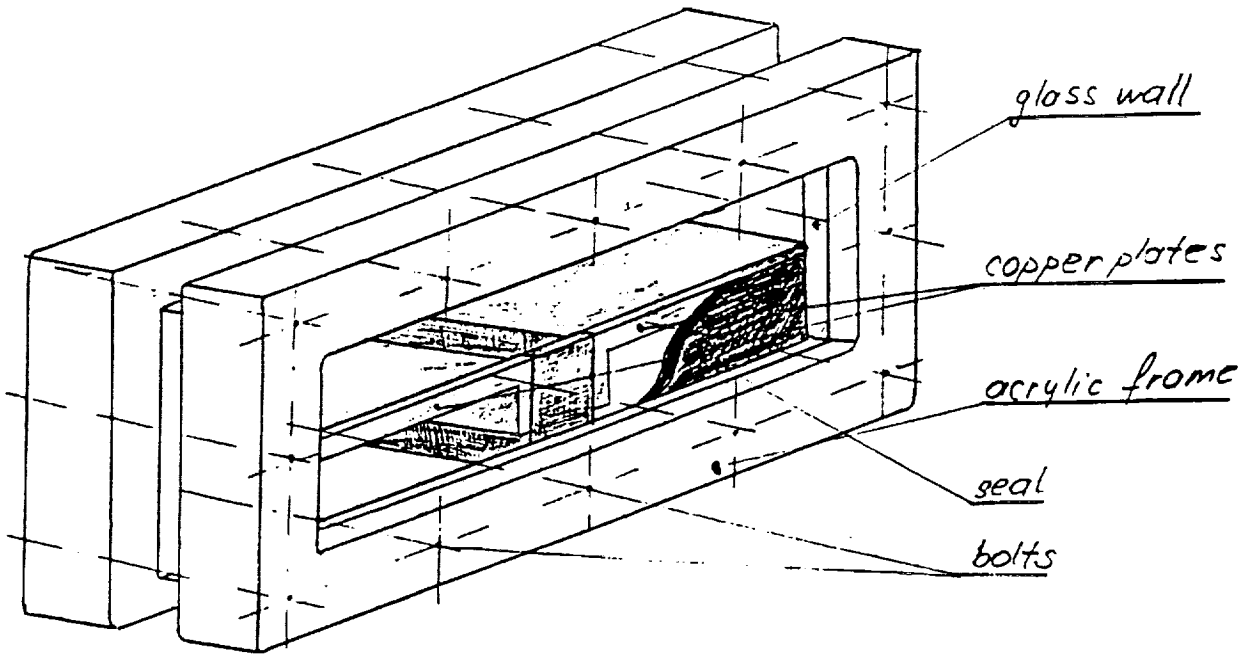

Figure 9: The Experimental Heat Pipe

The goal of this experiment was to measure temperatures in the rectangular heat pipe, which yields data for computer code or model assesment. In order to simulate proper boundary condition, the upper boundary, which simulates the centerlane of the heatpipe, was made of acrylic with low thermal conductivity. The lower boundary was made of copper plate, heated on the left side with two 1 square inch large patch heaters, and cooled on the right with counterstream cooling system, attached to a technical water tube system.

There are 7 thermo couples employed. Three on heaters side, three on cooled side and one of the top. In order to observe the experiment, the side walls were made out of water glass of high quality, 1/2" thick. The glass sides were cut on the water-cooled diamond circular saw-mill and finished with water-sander. Glass is sensitive to heat, and this has caused us many problems not only during the manufacturing process, but also during experiment.

In order to achieve proper results we have exposed the investigated system to high local heat fluxes. This has resulted in high temperature differences, which resulted in cracking of the glass walls. The additional problem was because of the high thermal conductivity of the glass, which can reach almost the value of the water. Due to this high thermal conductivity coefficient, we have got a condensation layer on the wall. This layer made a part of the temperature field unvisible, what can be observed

on the pictures taken. To solve the latter problem, the glass ought to be heated. We achieved that with use of the narrow patch heaters under the level of copper plates.

But this has even enhanced the local thermal stress in the glass and thuss the probability of glass breaking. Other "class" of problems were due to our cooling system. One of the demands while designing this experiment was the possibility to assemble and reassemble the heat pipe, therefore we could not employ epoxy glue for critical points. On the other hand, the precision criteria demanded for the bolted joints was not met due to lack of skills, therefore we settled for assembling with the use of RTV-silicon rubber. However, the side walls were still critical - there we have used rubber seals. But those seals required certain amount of pressure, applied toward the glass - copper plate junction, and that meant another possibility more for a crack of glass. The remedy for the thermal stress would be the use of the quartz glass - yet this material is even more sensitive to ordinary (pressure caused) stress then ordinary water-white glass we have used so far. To conduct described experiments without further delay we tried to find the optimum rate between the pressure, applied through tigtening bolts, and additional heat, added through side and main patch heaters. This was tedious process, however we have obtained some nice results.

The medium we have worked with ($C_2Cl_3F_3$, also known as Freon 113) was quite agressive, and reacted with sealant - silicon rubber RTV. This did not

cause us only troublesome assemblement and deassemblement of the heat pipe, but also left "yellow film" on the side walls.

A. HOLOGRAM TAKING TECHNIQUE

We have used the simple exposure technique with storage of comparison waves. This means that we have recorded the initial waves, i.e. the waves which pass through undisturbed system, and then observe the fringes, created via the plate shift of the measuring beam, penetrating through the disturbed object. The experimental setup (made by NRC /8/) is composed of the following elements:

1. LASER is the source of the coherent (i.e. single frequency) parallel beam, which is used for measurements. In first two experiments we have used red colored laser beam, i.e. He-Ne laser with 15mW power. This laser is small, easy to handle and air cooled, which makes it very handy for school purposes. In the last experiment we have used larger water cooled 4W maximum output Ar laser. Due to the fact that we needed coherent beam we were able only to use up to 240mW power. To got single frequency output the ethalon is employed. However, 240mW were used only while recording the hologram, the pictures were taken with 60-80mW power.
2. MIRRORS were used to elevate the beam on the level of experiment and to direction the splitted beams on the target - the hologram. With

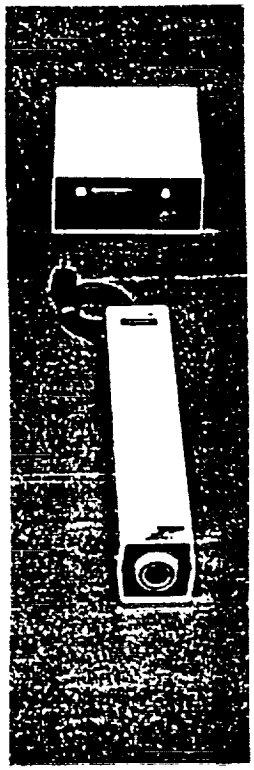

Figure 10: He-Ne laser 15 mW

mirrors adjustments we have also set the beam path to the same lenght.

3. SHUTTER is cruicial for recording good quality hologram. It function is exactly the same as with camera - it sets up the exposure time. For our experiments the best results were achieved by using exposure times around 1/5 sec. The effect of prolonged or too short exposure time can be corrected by adjusting the time of developing. By the means of developing time adjustments we can also control the level of greyness on the hologram. The fact is that brighter the hologram

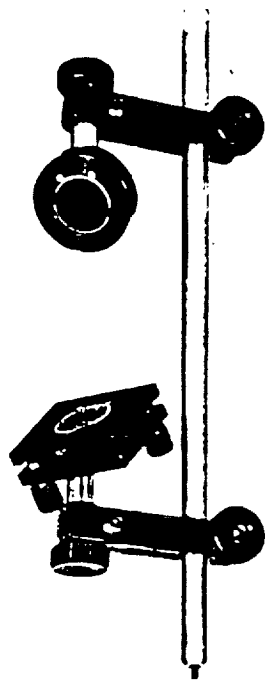

Figure 11: Mirrors

is, better our results will be. However, we may not lose the information, recorded on hologram. Therefore the best would be to record the hologram with quite a few darkness and then reduce it to be as bright as possible and yet not to lose any piece of information recorded. This is achieved with the use of ferrocide cianide, which bleached the hologram, but not remowed the shape, caused by light while taking the hologram.

4. BEAM SPLITTER splits the beam from the laser into two beams. One is used as a "measurement" beam, another is the reference beam.

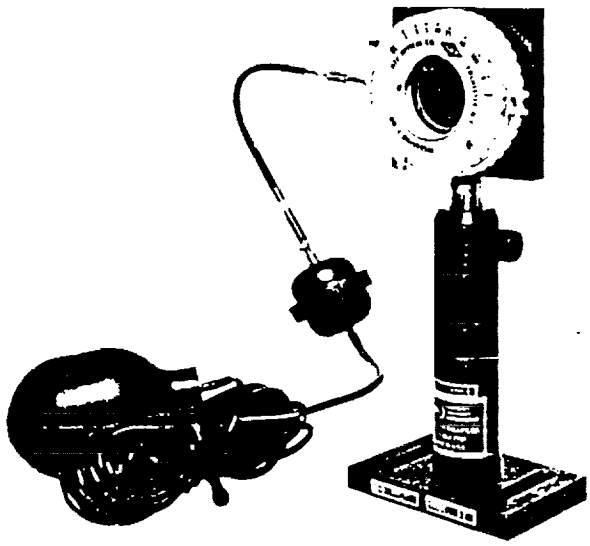

Figure 12: Shutter

Our beam splitter is a mirror with different degrees of reflection and transparence, which enables us to control the intensity of each beam by turning the beam splitter around its center. The other beam splitter (older one) was used as a filter for fine adjustments of intensity of measurement's beam.

5. SPATIAL FILTER was used to spread the beam on the wider area. Spatial filter is an apparatus, composed from objective lense 40:1, and a pinhole, which purpose is to homogeneous enlarge the beam crossection.
6. COLLIMATING LENSE is a lense which purpose is to direct the beam, which is spherically expanded from the objective lense, along z-axis

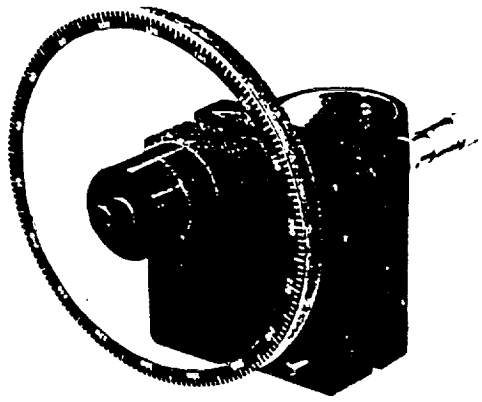

Figure 13: Beam Splitter

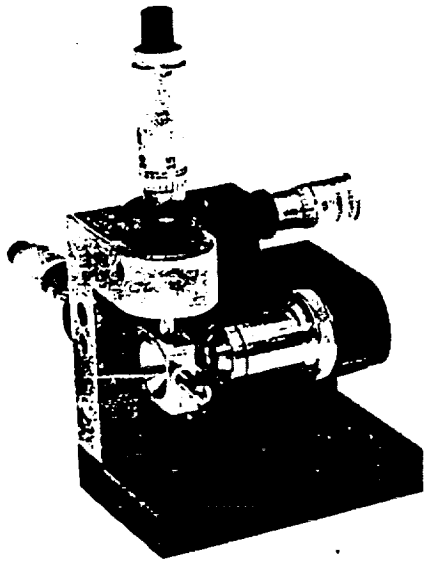

Figure 14: Spatial Filter

and thus form a "cylinder" or a measurement section. As the result, an experiment can be placed anywhere along the axis of the cylinder with no effect on the final hologram.

7. HOLDER consists of a steel housing, placed on a metal support and with a draining and filling system. Side walls are transparent - made out of water white glass. Part of a kit is also the hard-deck cover, which is used to protect undeveloped plate from being exposed to a light. The draining and filling system is used for developing the plate, after taking the hologram. The developer used was Kodak D-19 developer, fixer and indicator stop bath. The best results were achieved after developing for about 3 min rather than 5 minutes as recommended by Kodak Co.. If we were to work without the bleach, used to decolour the hologram, 30 - 45 seconds developing would probably be enough, however this is to be tested.

B. STEADY - STATE EXPERIMENT I

The goal of this experiment was to establish a relationship between the power, used for heating the heat pipe and the actual temparature in the flow field. This would enable us to controle and calibrate a computer code, written by Mr. Farrokh Issacci, Ph.D. student at UCLA, and understand the temperature pattern as well as critical heat points in the real heat pipe during operation.

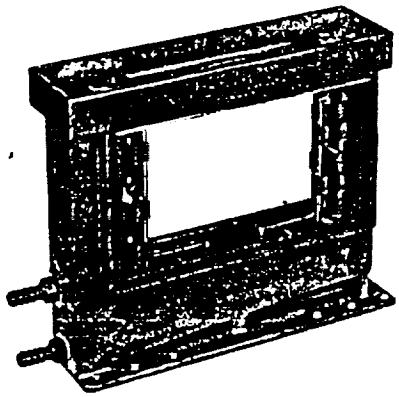

Figure 15: Holder

The heat pipe was divided into three sections A, B and C, each with three levels, as indicated in figure 16 . The results are tabulated and presented in form of graphs for each cross section A, B and C as a temperature as a function of position and power. The power meant is the input power to the patch heaters, which is not exactly the power, carried by the heat pipe, but gives us approximately right result. In the future we will calculate the real heat transfer from temeperatures known (i.e. known temperature gradient.) Interesting result is seen in the cross section B, where temperature along Y axis almost does not vary. To illustrate the development of temperature gradient, three photographs are attached, each for different power. To

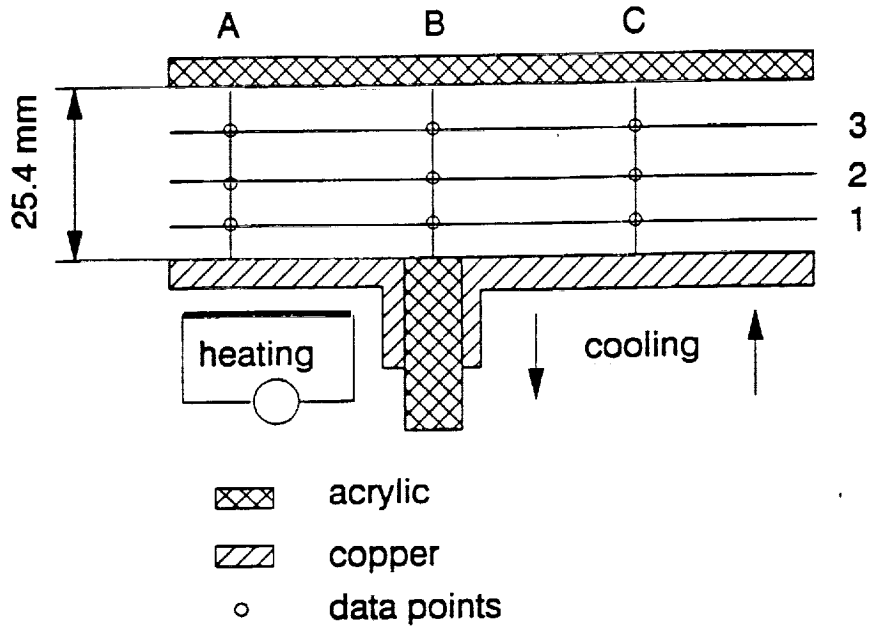

Figure 16: Measurement Points in the Heat Pipe Cross Section

enhance visibility of the last print, I have pointed them out by drawing black lines or dots in the middle of the fringe.

C. STEADY - STATE EXPERIMENT II

During first experiment the data recorded were obstructed by condensate, falling from the top and raising from the bottom. To enwiden the visible temperature field we have decided to remove the cork - acrylic simulated adiabatic boundary and let gas to expand all the way up. Since the housing is also made up from acrylic and since we added narrow patch

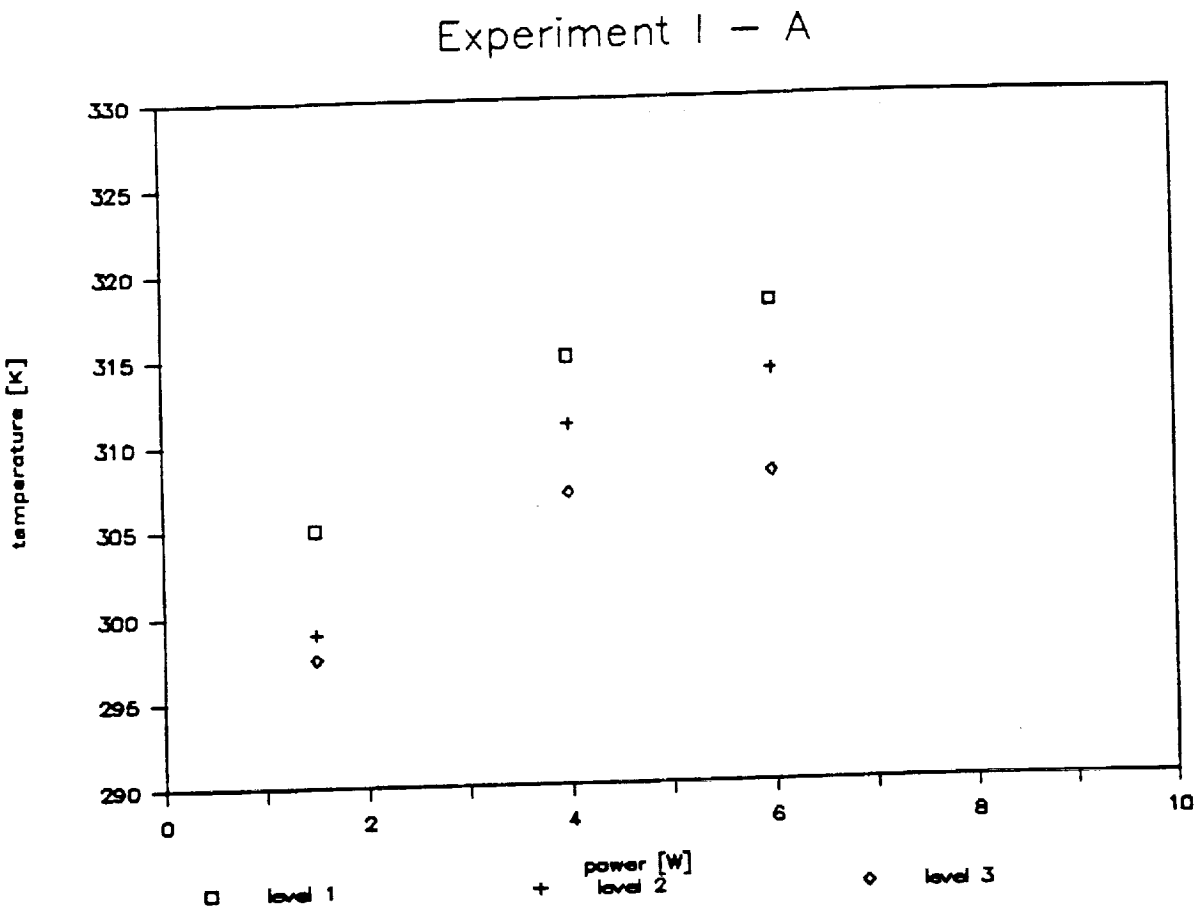

Figure 17: Temperature vs. Power in Cross Section A - Exp. I

heaters, warmed up to the pre-operational temperature, we did not lose in generality. The test section was now 13/16″ wide (before was 1/2″). The results were much clearer, which is seen also on the photographs enclosed.

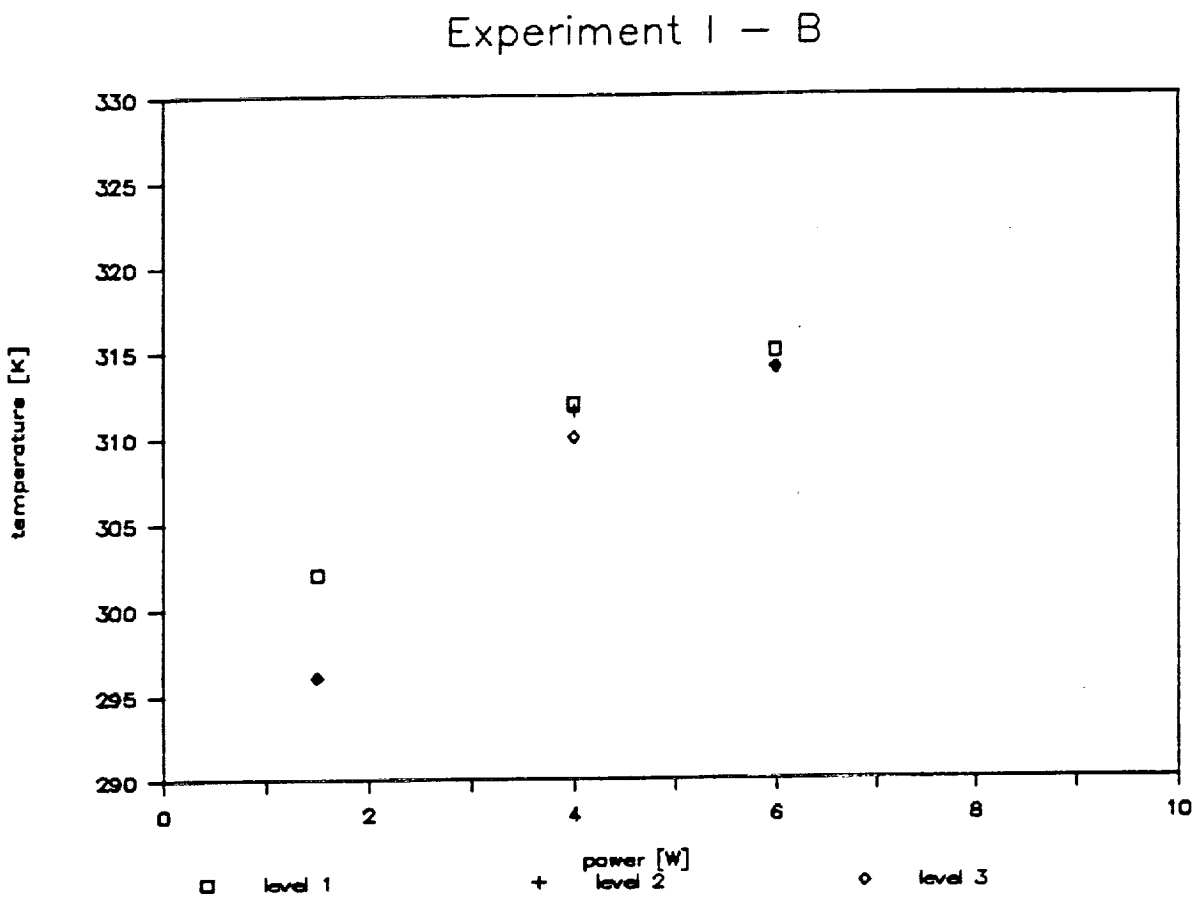

Figure 18: Temperature vs. Power in Cross Section B - Exp. I

Again, the results are presented in the form of graphs, showing the temperature as a function of power input. We can again observe smaller temperature gradient along vertical direction in section B as in section A.

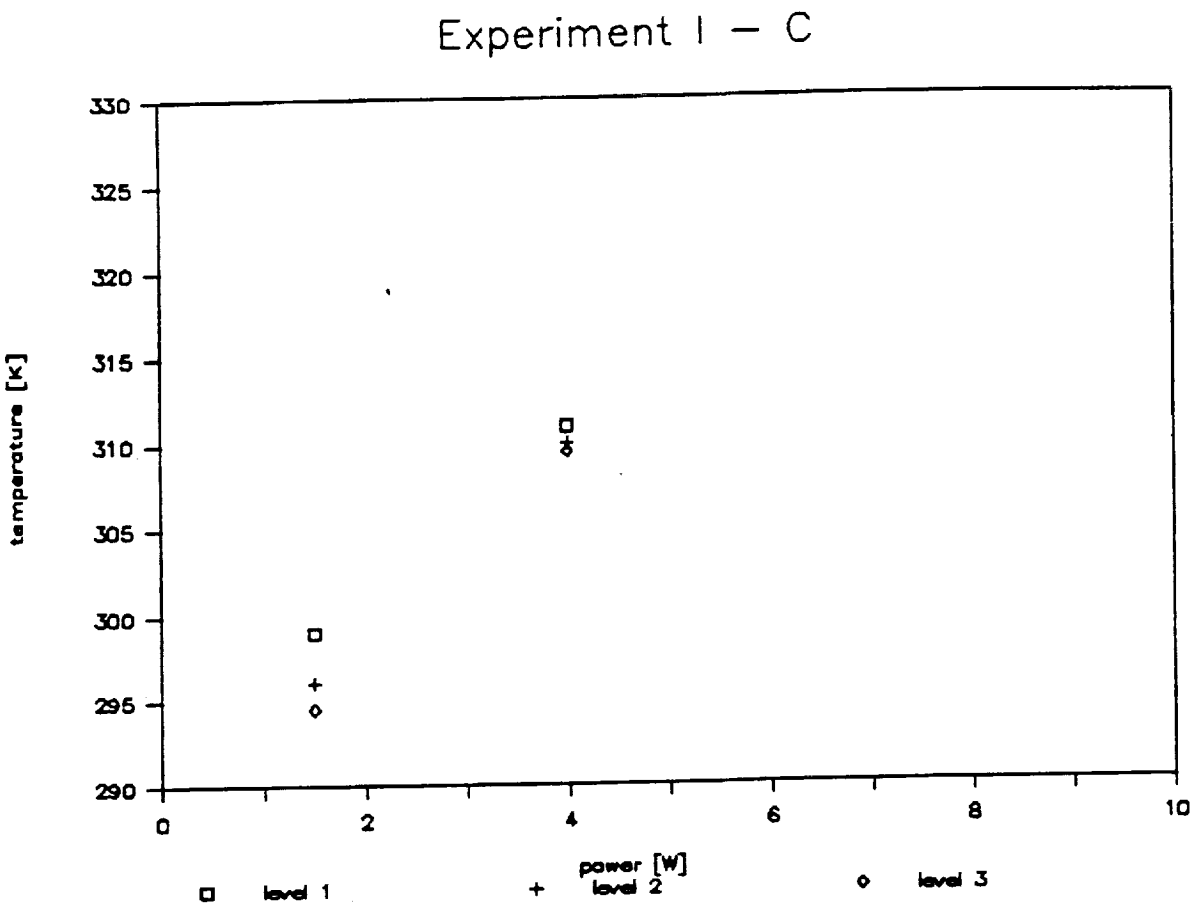

Figure 19: Temperature vs. Power in Cross Section C - Exp. I

D. TRANSIENT OPERATION

The goal of this experiment was to determine how fast the temperature field in the heat pipe achieves its steady- state value. In order to record this development, a series of photographs were taken, describing the development of the temperature field at a constant power. The width of the test section was again 13/16″, the power on heaters was 2.4 W. The graphs,

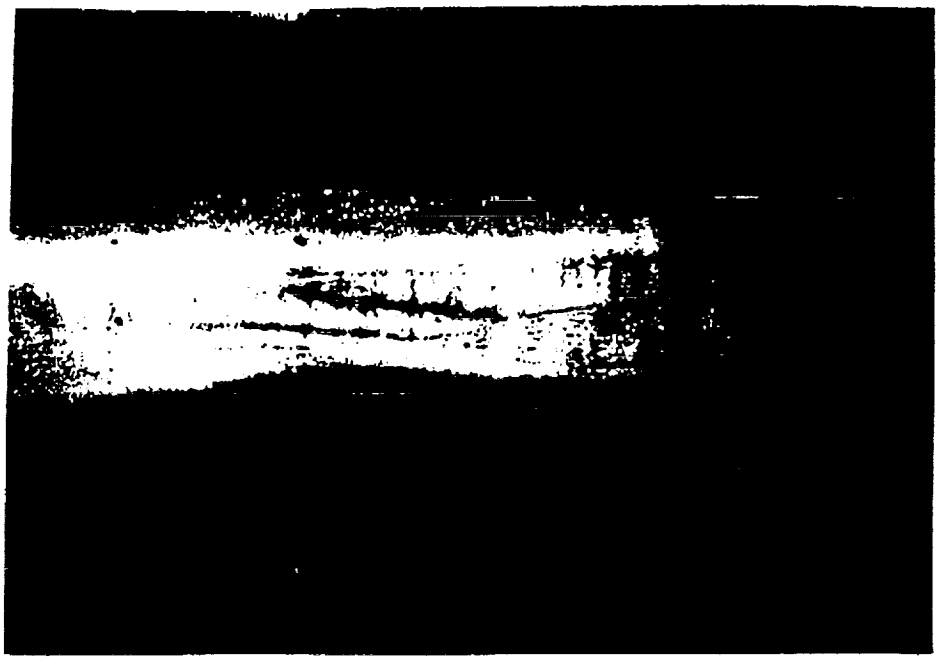

Figure 20: Fringes at Power = 1.5 W - Exp. I

describing section A, B, C as a function of position and time are attached as well as are of photographs at each step.

The result were obtained by calculating the temperatures by means of finite fringes, so the series of pictures taken represent the altering of temperature field as altering of finite tringes, therefore its appearance somwhat differ to the pictures, shown in previous sections. The graphs displayed show expected behaviour of temperature values while approaching the steady state. But note also the very slow mode of

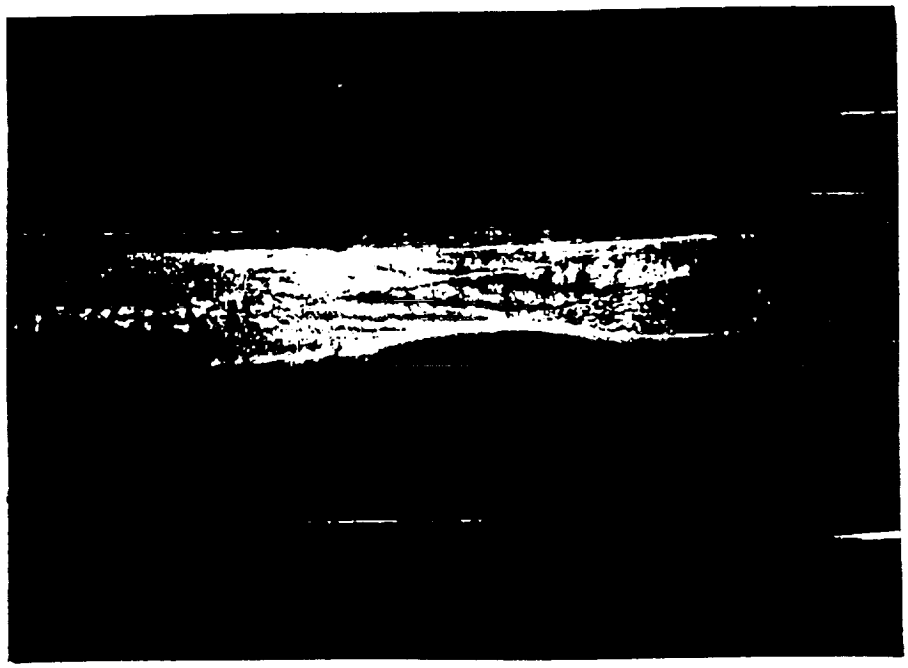

Figure 21: Fringes at Power = 4.0 W - Exp. I

establishing the steady state operation in heat pipes, which gives an oppurtunity to explore, how can this operation mode be achieved faster.

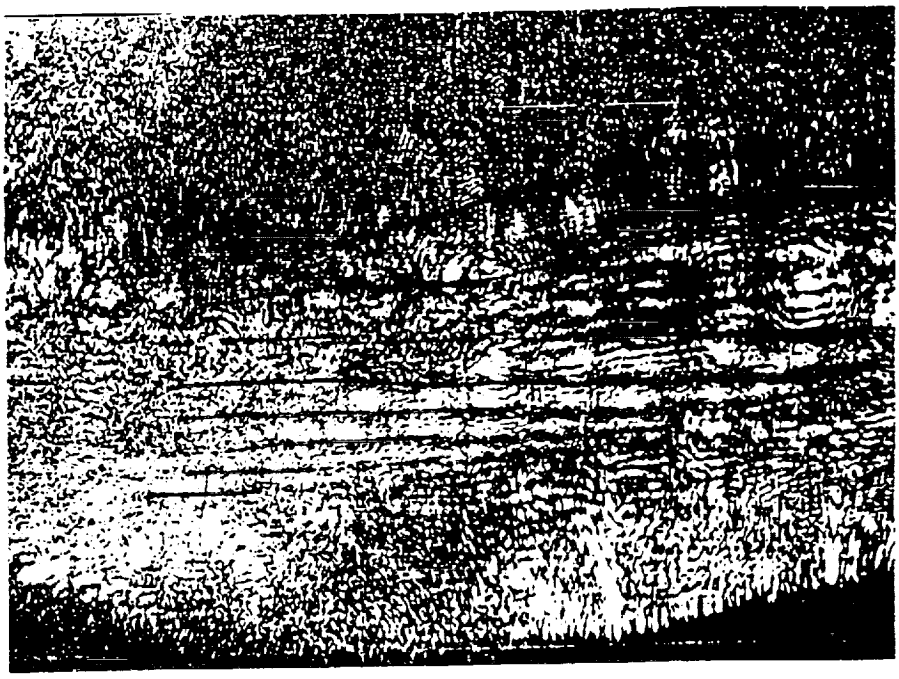

Figure 22: Fringes at Power = 6.0 W - Exp. I

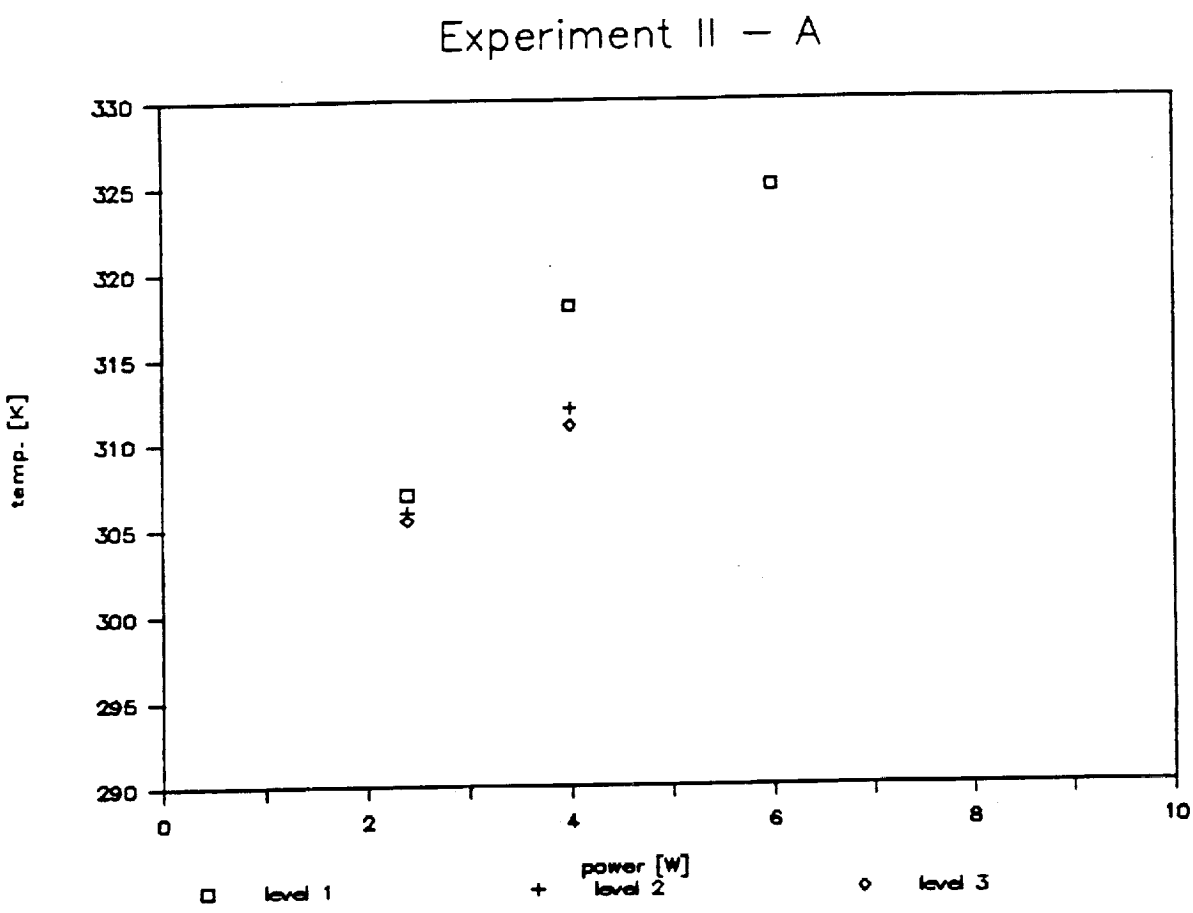

Figure 23: Temperature vs. Power in Cross Section A - Exp. II

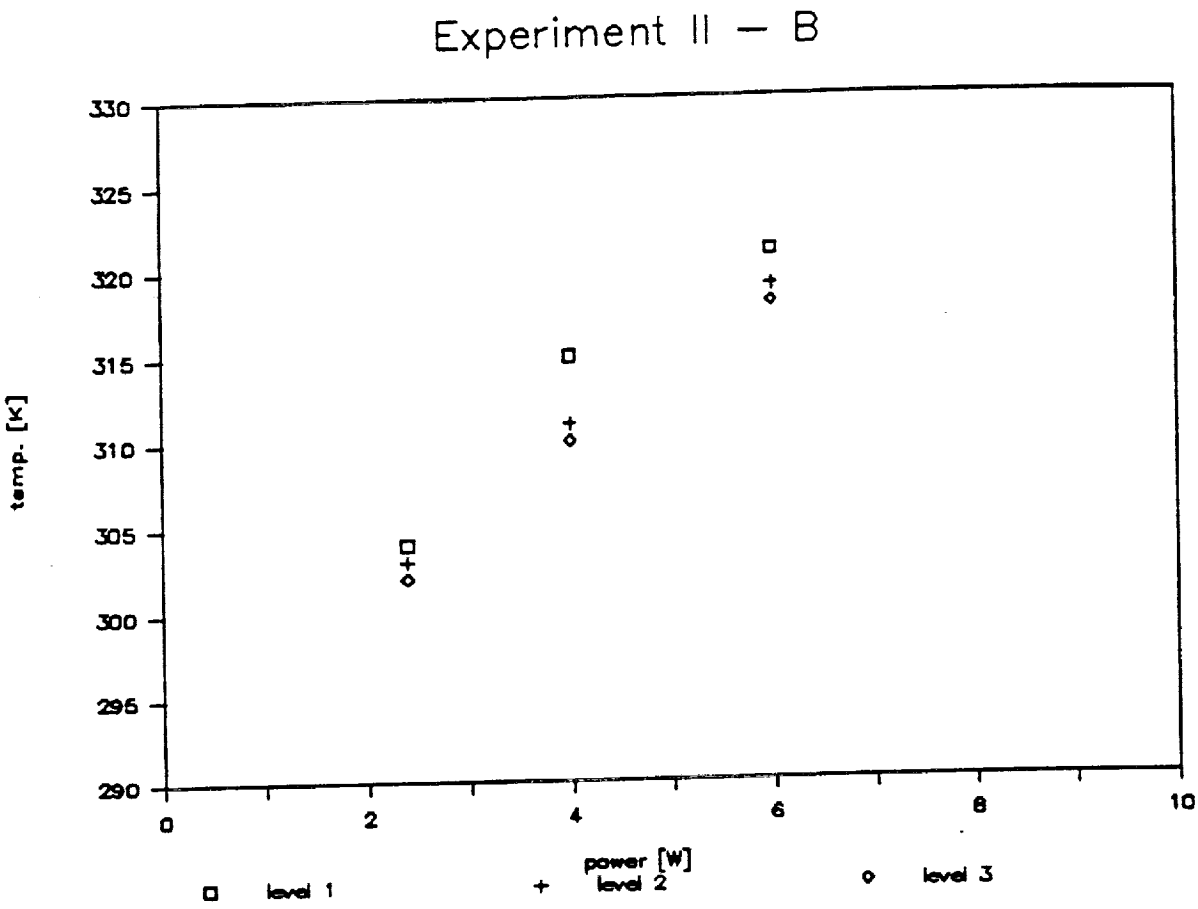

Figure 24: Temperature vs. Power in Cross Section B - Exp. II

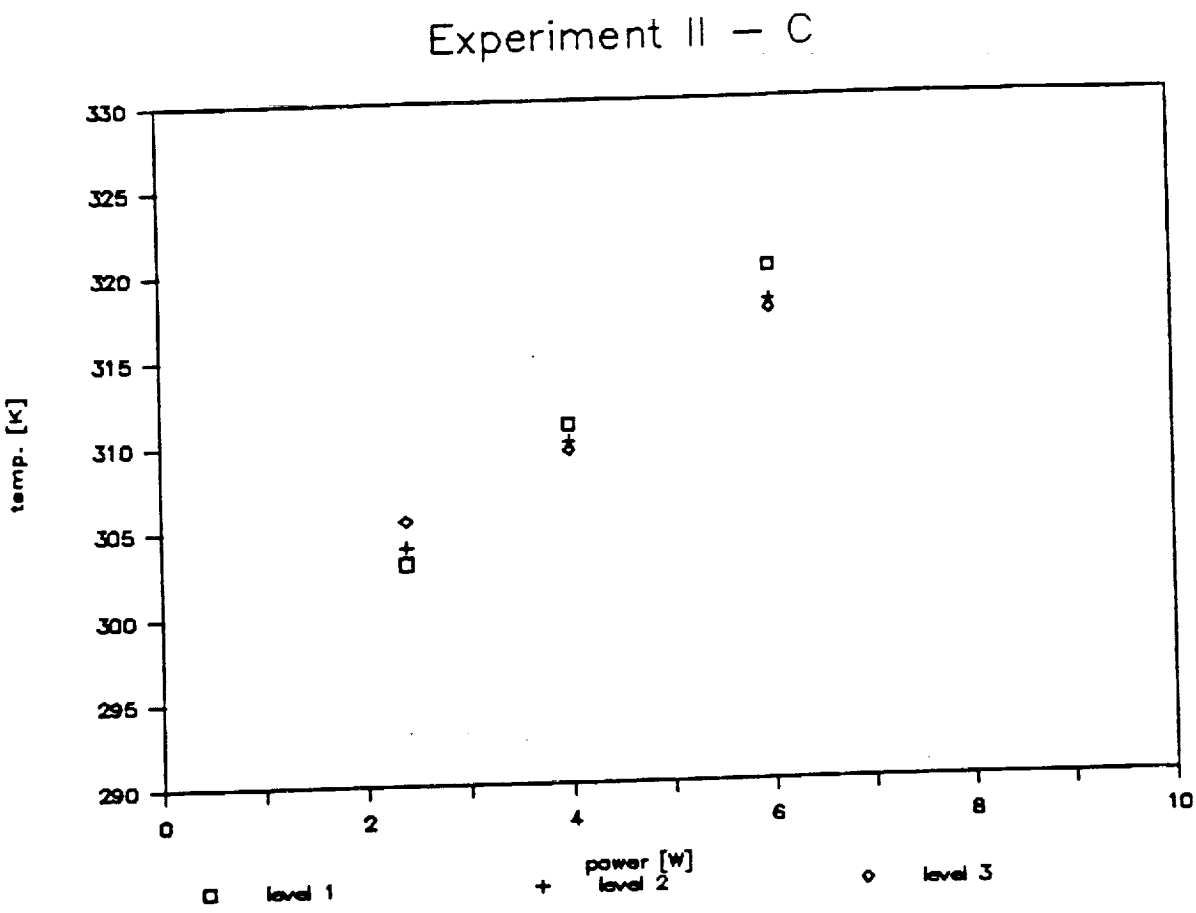

Figure 25: Temperature vs. Power in Cross Section C - Exp. II

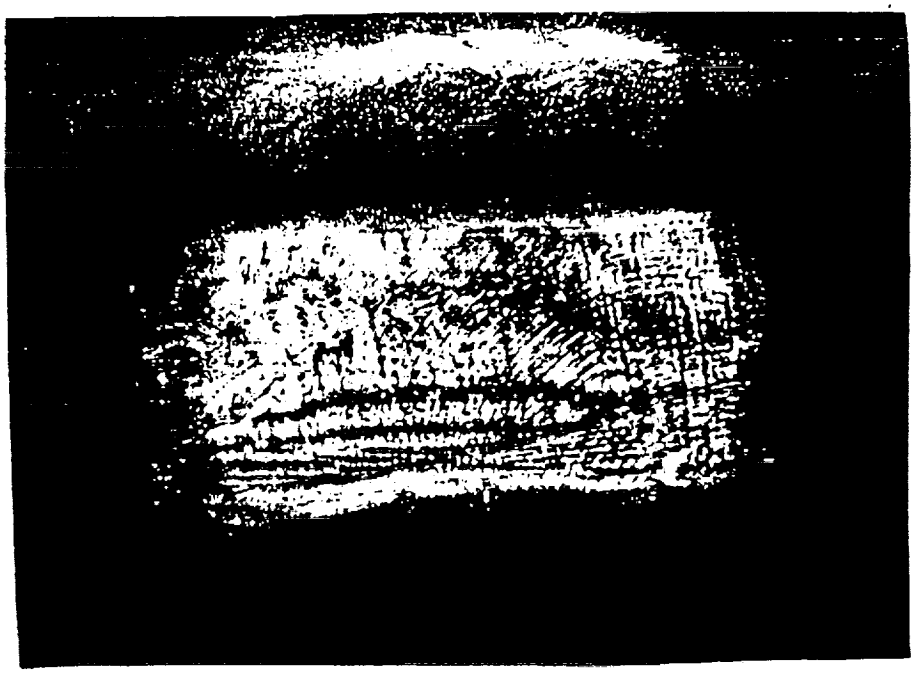

Figure 26: Fringes at Power = 2.0 W- Exp. II

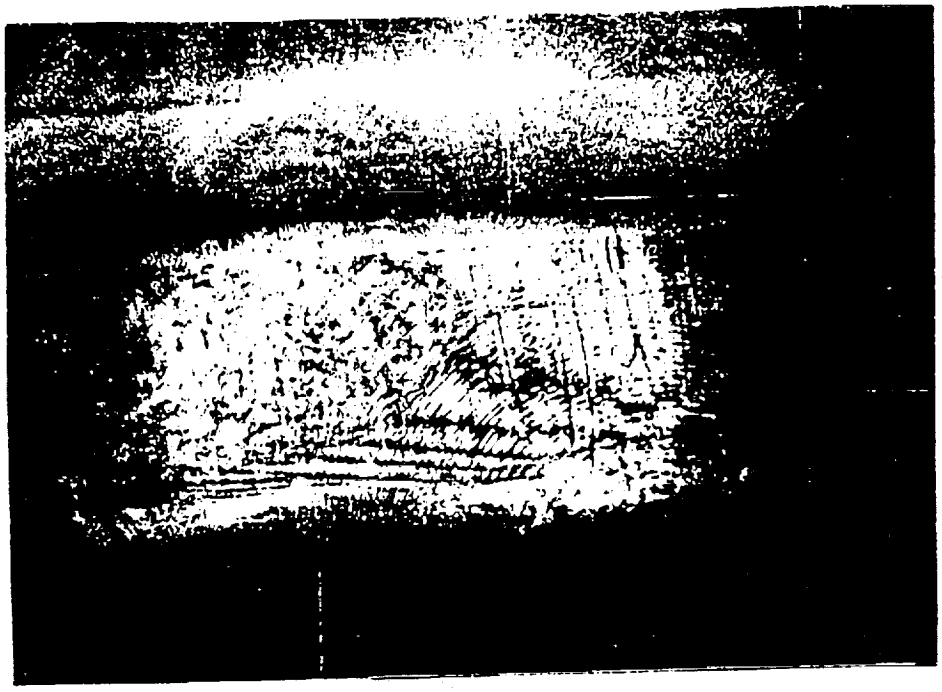

Figure 27: Fringes at Power = 4.0 W- Exp. II

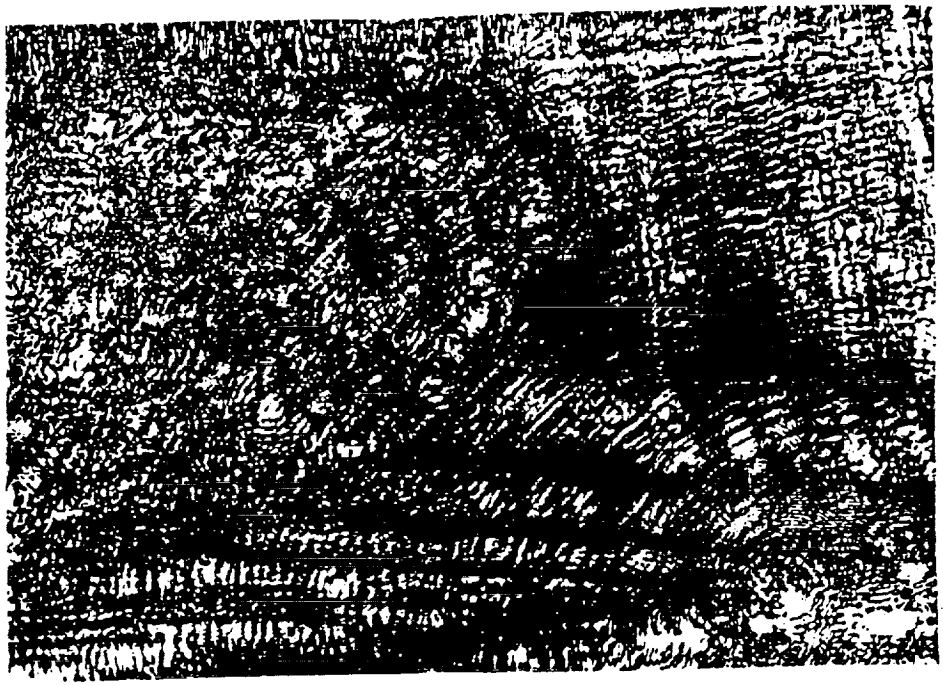

Figure 28: Fringes at Power = 6.0 W- Exp. II

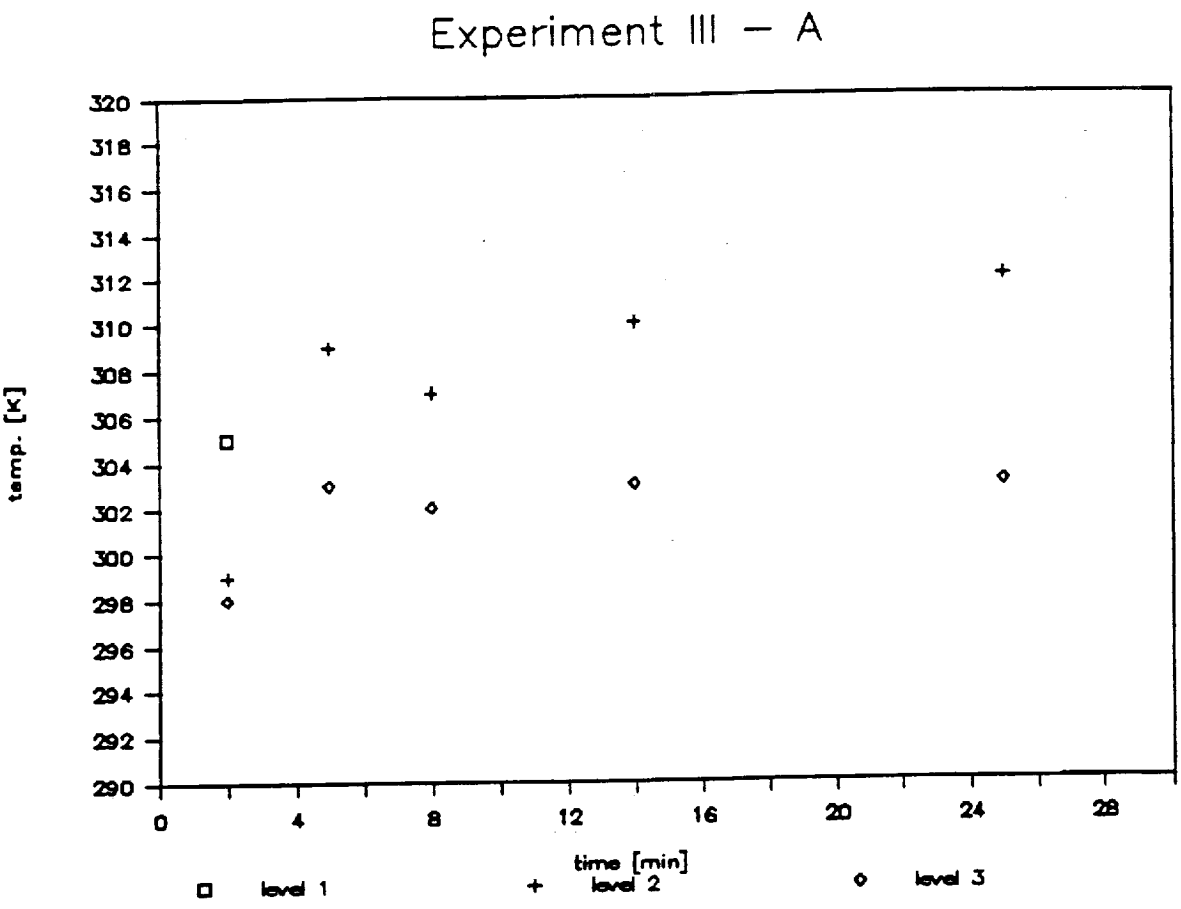

Figure 29: Temperature vs. Time at Constant Power = 2.4 W- Section A

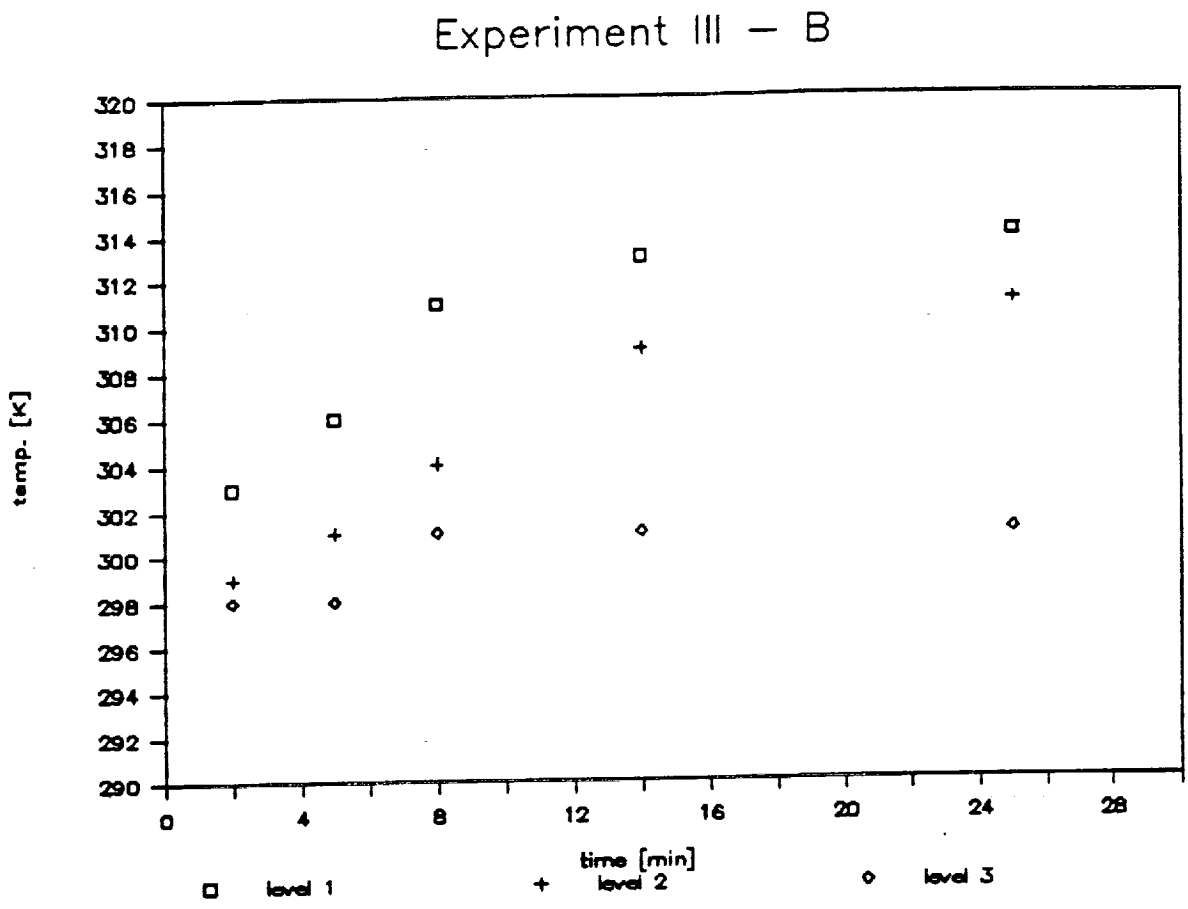

Figure 30: Temperature vs. Time at Constant Power = 2.4 W- Section B

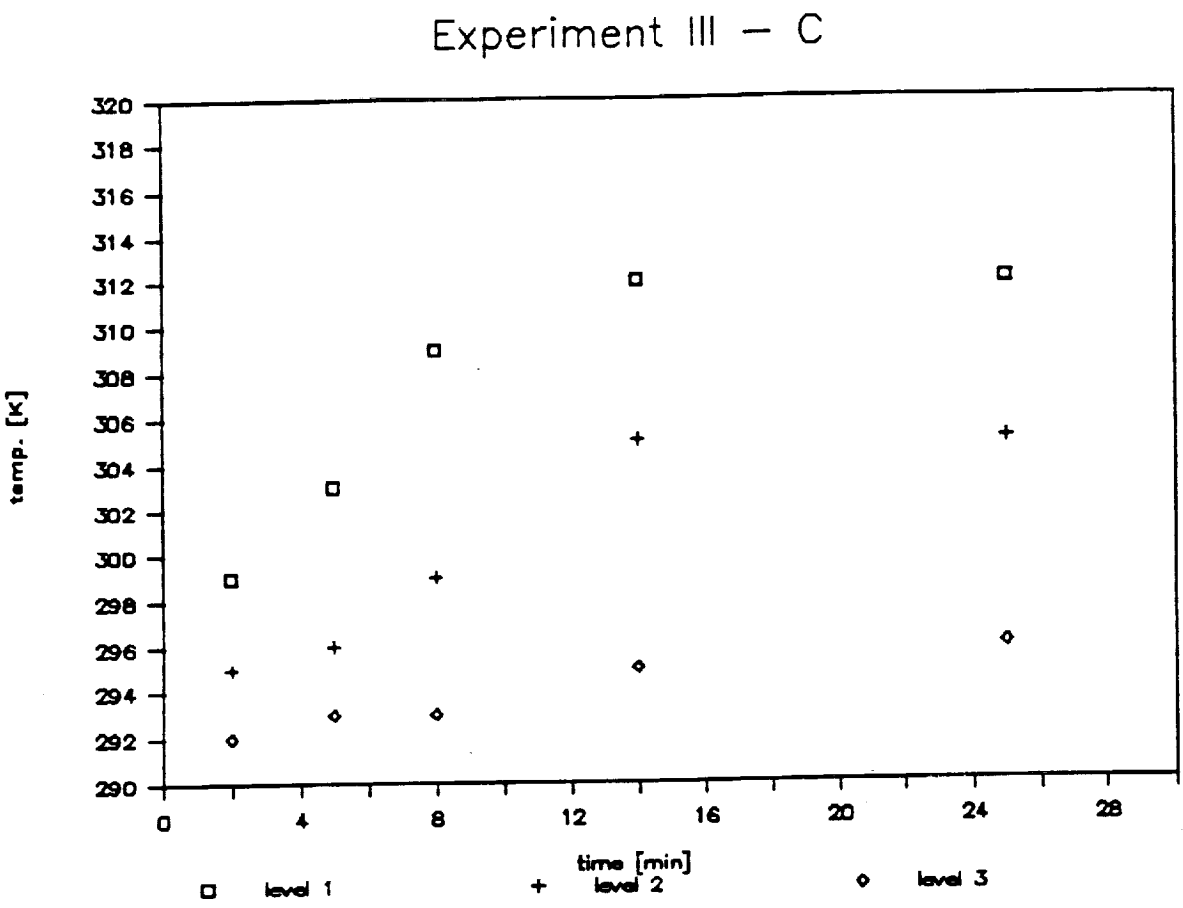

Figure 31: Temperature vs. Time at Constant Power = 2.4 W- Section C

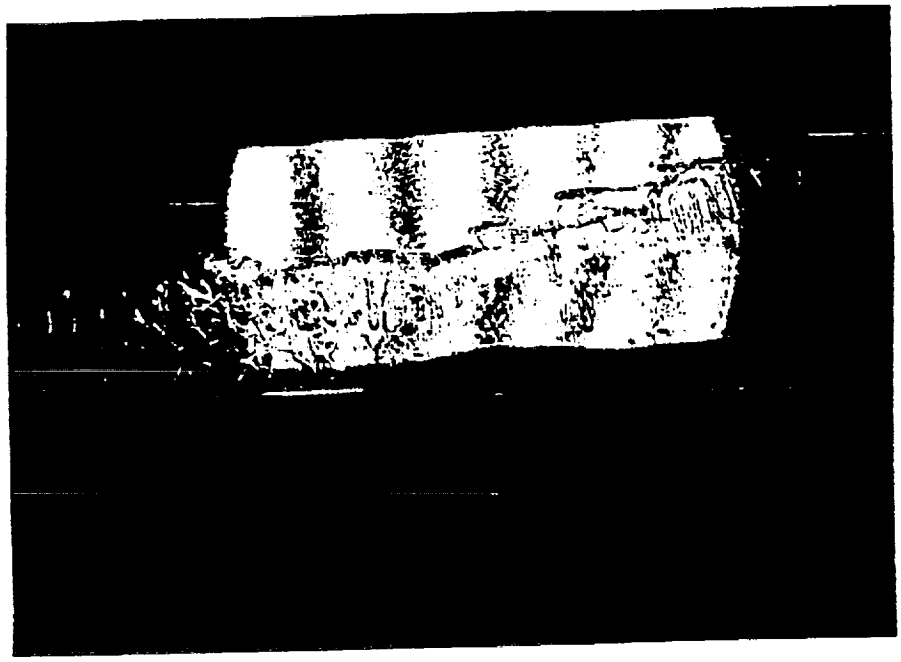

Figure 32: Fringes at Time = 0 min - Initial State

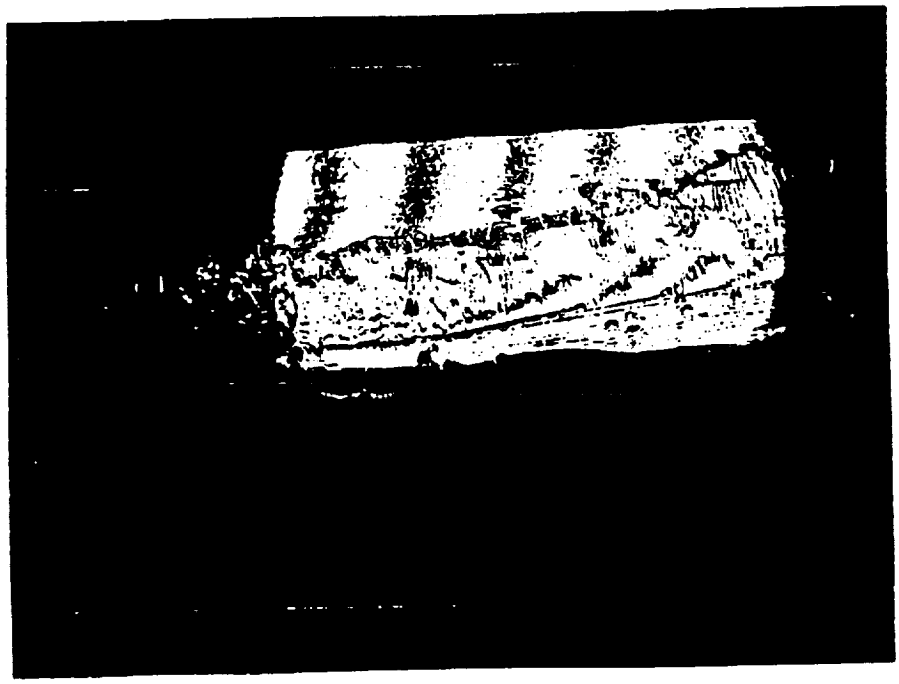

Figure 33: Fringes at Time = 2 min.

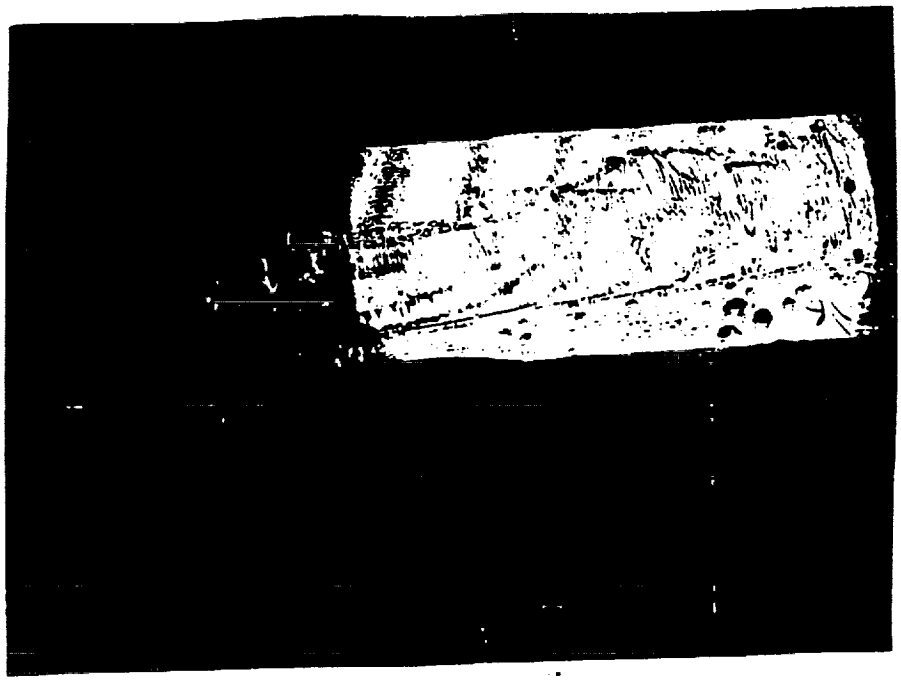

Figure 34: Fringes at Time = 5 min

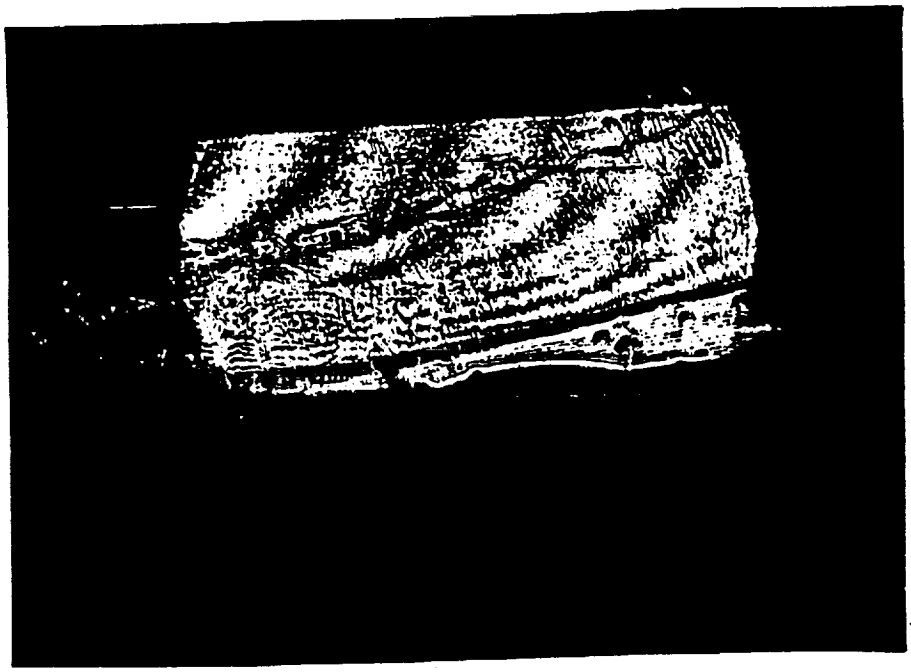

Figure 35: Fringes at Time = 8 min

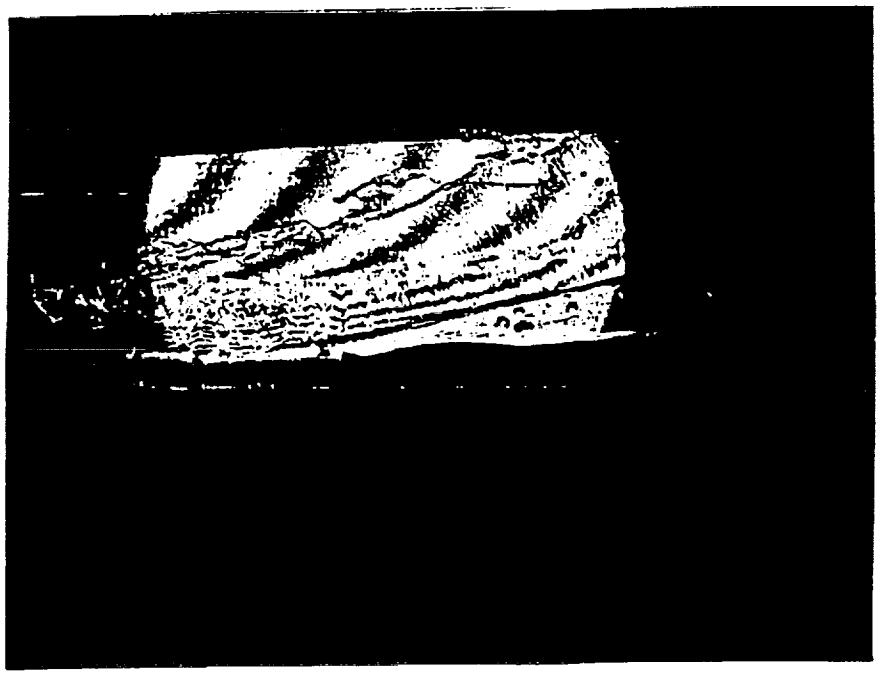

Figure 36: Fringes at Time = 14 min

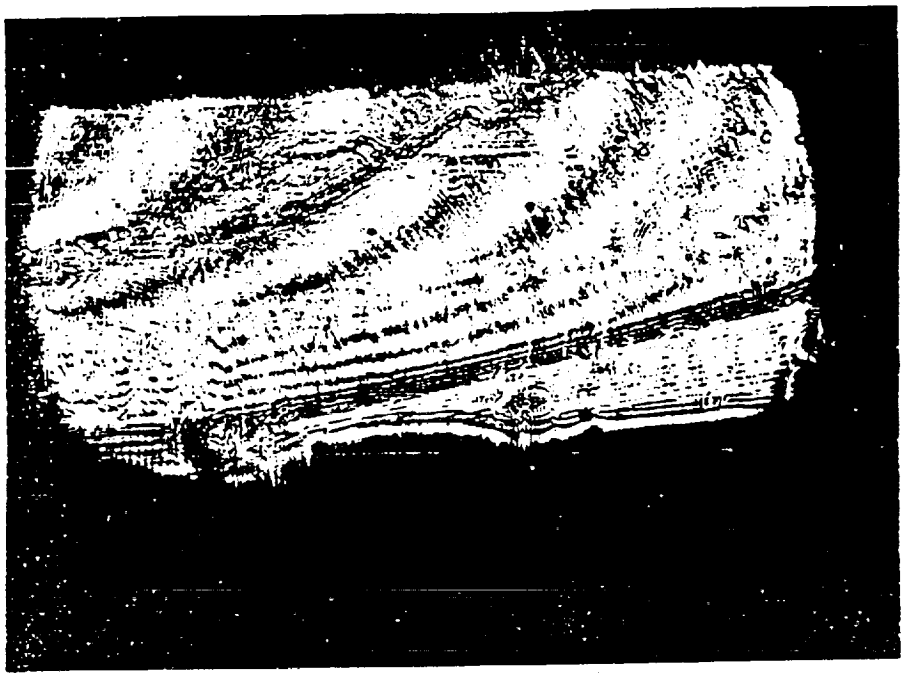

Figure 37: Fringes at Time = 25 min

Chapter IV

CONCLUSION

All three experiments can be included into single beam holography interferometry, however they were needed to conquer the techniques needed for using twin beam holography interferometry as well as understanding and calibrating the previouse mentioned computer code. The results shown qualitatively correspond to those, given in Mr. Issacci proposal, for the quantitative results, ought to be scaled and than compared.

A. FINAL REMARKS

Next step is obvious twin beam interferomety. As a cure for our cracking problem with the side windows, the acrylic windows should be used. Also, the quality of the pictures taken is going to be improved by using the appropriate developing and bleach techniques. In the future we will focus on behaviour of gas mixture in the heat pipe as well as buildup of concentration field in the heat pipe and thus predict and control operational mode of the heat pipe.

Chapter V

REFERENCES

/1/ Hauf, W. and Grigull, U., "Optical Methods in Heat Transfer" in Advances in Heat Transfer, 6, pp 134-366, 1970.

/2/ Issacci, F., "Experimental and Theoretical Investigation of the Unsteady Heat and Mass Transfer in Heat Pipes", Ph.D. Dissertation Proposal, UCLA 1988.

/3/ Gaugler, R.S., "Heat Transfer Device", US Patent No. 2,350,348, 1942.

/4/ Grover, G.M., Cotter, T.P., Erickson, G.F., "Structures of Very High Thermal Conductance", J. Appl. Phys., 36, No 6, pp 1990-1991, 1964.

/5/Cotter, T.P., "Theory of Heat Pipes", LA - 3246 - MS, 1965.

/6/ Mayinger, F., Panknin, W.,"Holography in Heat and Mass Transfer", Proc., 5 &th.International Heat Transfer Conf., VI, pp.28-43, Japan, 1974.

/7/ Panknin, W.,"Eine Holographische Zweiwellenlangen Interferometrie zur Messung uberlagetr Temperatur- und Konzentrazionsgrenzschichten", Ph.D. Dissertation, Technischen Universitaet Hannover, F.R.Germany, 1977.

/8/ Newport Corporation 1983/84 Catalog, 2nd Edition

/9/ Catton, I., Issacci, F., Heiss, A.,"Use of Optical Methods for Studyof the Dynamic Behavior of Heat Pipes", Proc., 1st world Conf. on Exp. Thermodynamics, Fluid Mechanics and Heat Transfer, Yugoslavia, 1988.